Chen *et al. Microstructures* 2022;2:2022012
DOI: 10.20517/microstructures.2022.10

Microstructures

Review

Open Access

Check for updates

Design and manufacture of high-performance microbatteries: lithium and beyond

Feiyang Chen, Zheng-Long Xu

State Key Laboratory of Ultraprecision Machining Technology, Department of Industrial and Systems Engineering, The Hong Kong Polytechnic University, Hung Hom, Hong Kong, China.

Correspondence to: Dr. Zheng-Long Xu, State Key Laboratory of Ultraprecision Machining Technology, Department of Industrial and Systems Engineering, The Hong Kong Polytechnic University, 11 Yuk Choi Rd, Hung Hom, Hong Kong, China. E-mail: zhenglong.xu@polyu.edu.hk

How to cite this article: Chen F, Xu ZL. Design and manufacture of high-performance microbatteries: lithium and beyond. *Microstructures* 2022;2:2022012. https://dx.doi.org/10.20517/microstructures.2022.10

Received: 29 Apr 2022 **Accepted:** 24 May 2022 **Published:** 30 May 2022

Academic Editor: Jun Chen **Copy Editor:** Fangling Lan **Production Editor:** Fangling Lan

Abstract

The accelerated development of miniaturized and customized electronics has stimulated the demand for high-energy microbatteries (MBs) as on-chip power sources for autonomous state operations. However, commercial MBs with thin-film configurations exhibit insufficient energy and power density due to their limited active materials and sluggish ion diffusion kinetics. In order to simultaneously enhance electrochemical performance and maintain low-cost production, efforts have been devoted to constructing three-dimensional battery architectures. This review summarizes the state-of-the-art progress in designing and fabricating microelectrodes for microbattery assembly, including the top-down etching and bottom-up printing techniques, with a particular focus on elucidating the correlations between electrode structures, battery performance, and cost-effectiveness. More importantly, advancements in post-lithium batteries based on sodium, zinc and aluminum are also surveyed to offer alternative options with potentially higher energy densities and/or lower battery manufacturing costs. The applications of advanced MBs in on-chip microsystems and wearable electronics are also highlighted. Finally, conclusions and perspectives for the future development of MBs are proposed.

Keywords: Microbatteries, lithium-ion batteries, post-lithium batteries, etching and printing techniques, microelectronics

INTRODUCTION

With the relentless development of microelectronics, including medical implantable chips, microrobots, wearable devices, and wireless sensors, miniaturized energy storage devices have become indispensable in enabling their autonomous state operations[1,2]. To shift from disposable or off-chip power suppliers to integrated and rechargeable ones, micro-supercapacitors (MSCs) and microbatteries (MBs) are considered promising alternatives[3,4]. MSCs possess the merits of high power density (10-1000 W cm^{-3}) and long cycle life (up to 10,000 cycles) through the fast absorption/desorption of electrolyte ions or a Faradic reaction at the electrode surfaces. Nevertheless, the energy density of MSCs (0.01-10 mWh cm^{-3}) is orders of magnitude lower than that of MBs (20-200 mWh cm^{-3})[5]. In this context, MBs have taken priority as the built-in power supplies for next-generation microelectronics[6].

In general, rechargeable batteries consist of cathodes, anodes, and separators with electrolytes inserted between them[7,8]. During charging and discharging, charge carriers shuttle forwards and backwards between the anode and cathode materials without causing deleterious changes in the electrolytes (as shown in Figure 1)[9]. Commercial lithium-ion batteries (LIBs) with a graphite anode and lithium transition metal oxide cathode have dominated the battery market for decades due to their high energy density, wide affordability, reduced memory effect, and low cost[10-12]. A conventional LIB cell is usually prepared by mixing the electrode slurries, tape casting on current collectors, winding the cell components, packing the laminated electrodes and separators into the pouch/coin cell, and then finally injecting the liquid electrolyte. Commercial MBs are essentially microscale versions of their bulk counterparts with laminated two-dimensional (2D) thin-film electrodes. Although this straightforward strategy has accelerated the commercialization of Li-ion MBs, the attainable energy and power densities are significantly decreased because the material loadings are also downscaled as a result of the constrained footprint area. Increasing the thickness of the laminated electrodes has been proposed for improving the energy density of MBs; however, such thick geometries suffer issues associated with tortuous charge transfer pathways and sluggish reaction kinetics, leading to deteriorated power performance. Recent developments in three-dimensional (3D) MBs have been used to achieve higher energy density and power capability concurrently while maintaining minimal spatial footprints. These 3D electrode architectures present large surface-to-volume ratios to maximize the mass loading and shorten the ion diffusion pathways. Several methods, such as wet or dry etching, photopatterning, and electrodeposition, have been developed to build feasible 3D electrodes for MBs[13].

Li-ion MBs are now taking the lead in powering microelectronics due to their mature manufacturing techniques and reliable electrochemical performance[14,15]. Nevertheless, the limited and unevenly distributed lithium resources in the Earth's crust, as well as the usage of toxic cobalt, have induced concerns regarding the sustainable supply of LIBs for large-scale applications in the future. As a result, alternative MBs based on lithium-free technologies that address these deficiencies have been explored in recent years[16]. Alkali-ion batteries (i.e., Na^+) with abundant resources have been explored for the possible substitution of lithium. Additionally, aqueous zinc-ion batteries have been investigated due to their merits of using non-flammable and inexpensive aqueous electrolytes and high-volumetric-capacity Zn metal (5854 mAh L^{-1} compared to 2061 mAh L^{-1} for Li metal)[17]. Similarly, Al redox electrochemistry, with the largest volumetric capacity of 8045 mAh L^{-1}, has been demonstrated to cycle in an aqueous electrolyte for safe MBs[18]. Therefore, post-lithium MBs hold significant promise for the enrichment of miniaturized power sources.

To date, several reviews have summarized the fabrication techniques for 3D microelectrodes and the optimization of scalable techniques, like 3D printing for industrial compatibility[19,20]. However, two fundamental features arising from recent developments have not been fully explored, namely, the robust

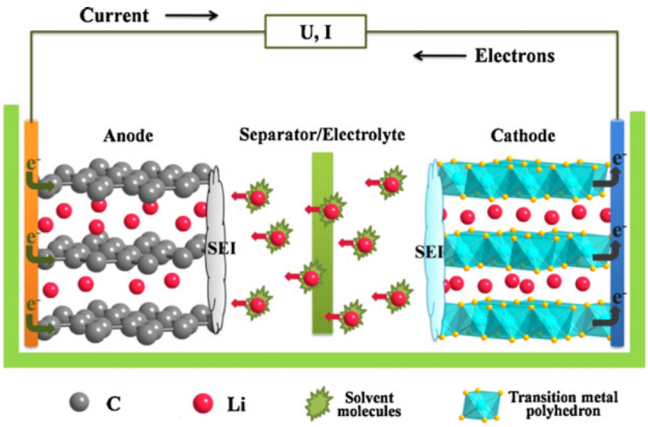

Figure 1. Schematic illustration of rechargeable battery working mechanism taking a LIB as an example (charging) (reproduced with permission[9]. Copyright 2012, Elsevier). LIB: Lithium-ion battery.

design principles of 3D electrode fabrication regarding the specific challenges for Li-MBs and the opportunities of post-lithium MB systems. Herein, this review discusses these aspects with an emphasis on the technical fundamentals for miniaturized fabrication, the necessity to shift from 2D to 3D electrode design, the advances in Li-free MBs and the cutting-edge applications of MBs. We expect this review to attract more attention to the study of MBs and foster a solid foundation for the mass fabrication of high-performance MBs.

TECHNIQUES FOR MANUFACTURING MICROELECTRODES

In contrast to traditional battery systems, the fabrication of MBs is delicate and requires meticulous preparation, as well as the compactness and compatibility of various cell components, including electrode materials and electrolytes[14,21]. The realization of high-energy MBs relies on the design and construction of miniaturized electrodes. The ever-developing fabrication techniques can be classified into two categories, namely, "top-down" etching methods (i.e., photolithography, laser engraving and plasma etching) and "bottom-up" printing techniques (i.e., screen printing, inkjet printing and 3D printing). The advantages and challenges of each technique are summarized in Figure 2 and discussed in detail as follows.

Etching technique

Etching involves chemically or physically removing the unwanted parts of bulky substrates to leave the interdigitated patterns. It has been considerably utilized in micro/nanoelectronic manufacturing fields with the advantages of high resolution and design flexibility and simple operation. Representative etching methods, including photolithography, laser engraving, and plasma etching, have been fully leveraged in the machining of microelectrodes.

Photolithography

Photolithography, also known as ultraviolet (UV) lithography[22], is one of the most mature patterning technologies for MB fabrication[23] and is based on photochemical reaction and developing processes. Typically, by applying UV light to a photoresist polymer through a photomask pattern, the positive area (covered by the mask) is soluble in the developer solution while the negative area (exposed to UV light) is retained[14,23]. Therefore, the unexposed pattern will be removed to form an engraving pattern for the following deposition of current collectors and active materials. Pt or Au, as a current collector, is usually covered on the pattern through physical vapor deposition or magnetic sputtering, followed by the electrochemical plating or atomic layer depositing of active materials. The shape, resolution, and height of

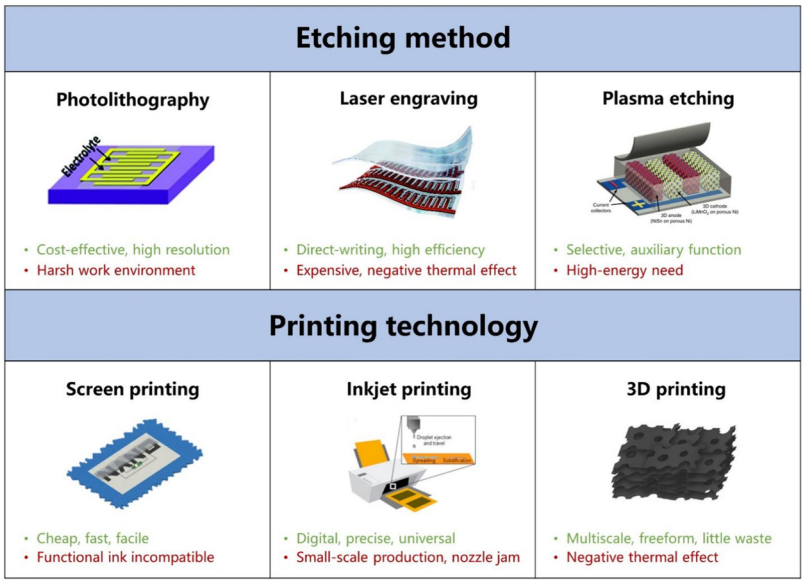

Figure 2. Summary of common technologies used in MB fabrication. Photolithography (reproduced with permission[24]. Copyright 2014, Royal Society of Chemistry). Laser engraving (reproduced with permission[28]. Copyright 2018, Royal Society of Chemistry). Plasma etching (reproduced with permission[31]. Copyright 2013, Nature Publishing Group). Screen printing (reproduced with permission[35]. Copyright 2016, Wiley-VCH). Inkjet printing (reproduced with permission[40]. Copyright 2017, Elsevier). 3D printing (reproduced with permission[46]. Copyright 2018, Wiley-VCH). MB: Microbattery.

the photolithographed electrodes are tailorable by engineering the photomask patterns and lithography parameters.

In order to maximize the energy density of photolithographed electrodes on a limited area, increasing the number of interdigital fingers by minimizing the finger width has been demonstrated to be effective. The energy density of a deposited graphene oxide electrode could be improved to ~3.6 mWh cm^{-3}[24] by increasing the number of fingers from 8 to 32 and narrowing the finger width from 1175 to 219 μm. The photoresist is usually used as the soft sacrificial material for patterning during photolithography [Figure 3A]. A modified photoresist was recently developed as a solid electrolyte or electrode for MBs. For example, SU-8 is the most representative negative photoresist to pattern high spatial resolution and aspect ratio structures. By adding a lithium perchlorate salt ($LiClO_4$) to the crosslinked SU-8 structures, a solid electrolyte was obtained and exhibited a high ionic conductivity of 52 μS cm^{-1} and a wide electrochemical window of 5 V[25]. By photopatterning the modified SU-8 photoresist on Si nanorod arrays, 3D MBs consisting of a Si//solid electrolyte//$LiNi_{0.8}Co_{0.15}Al_{0.05}O_2$ (NCA) cell configuration were achieved and delivered a peak discharge capacity of 5.2 mWh cm^{-2} and a reversible capacity of 1.6 mWh cm^{-2} at the 100th cycle[26]. The photolithographed SU-8 photoresist was also directed carbonized into carbon microelectrodes[27], and the arrayed carbon structure enabled a high Li-ion storage capacity of 596 mAh g^{-1} after 165 cycles.

In summary, photolithography is a powerful micromanufacturing technique that possesses high dimensional flexibility and photoresist material design, thus enriching the MB fabrication possibilities. However, it is difficult to obtain thick 3D structures for high-loading microelectrodes using this method. In addition, the relatively complicated process steps and the demands of special operating environments, such an ultraclean room, restrict the ubiquitous application of photolithography in microelectrode fabrication.

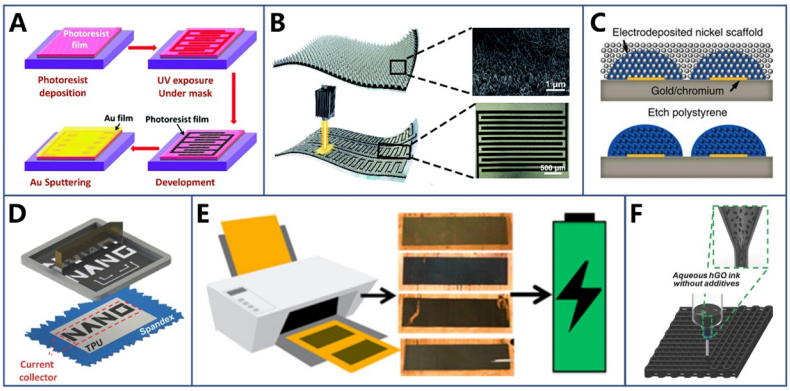

Figure 3. (A) Schematic illustration of interdigitated structures via photolithography (reproduced with permission[24]. Copyright 2014, Royal Society of Chemistry). (B) Schematic illustration of MBs produced via laser engraving (reproduced with permission[28]. Copyright 2018, Royal Society of Chemistry). (C) Formation of nickel scaffold via plasma etching (reproduced with permission[31]. Copyright 2013, Nature Publishing Group). (D) Fabrication of Zn-Ag_2O MB via screen printing (reproduced with permission[35]. Copyright 2016, Wiley-VCH). (E) Schematic illustration of inkjet printing process (reproduced with permission[40]. Copyright 2017, Elsevier). (F) 3D printing process (reproduced with permission[46]. Copyright 2018, Wiley-VCH). MB: Microbattery.

Laser engraving

Laser engraving directly writes microelectrodes via the heating and evaporating of electrode materials under laser beams. The operating parameters, including the laser fluence, scribing route, and scan speed, can be used to control the delicate electrode microstructures. In addition, laser engraving is contactless, facile, substrate independent, and photomask free, thus even enabling microfabrication on flexible media.

The laser beam can work as both a scavenger for patterning and a heating source for carbonization. For example, Lai *et al.* developed a flexible rechargeable Zn//MnO_2 MB consisting of Zn@Ni nanocone array anodes and 3D MnO_2@Ni nanocone array (NCA) cathodes[28]. The NCA films were laser engraved by a commercial laser with a wavelength of 355 nm to acquire an interdigital structure, and the MnO_2 and Zn active materials were then electrodepositedN on each side, respectively [Figure 3B]. The laser size could be narrowed to ~10 μm, thereby enabling the design of compacted interdigital arrays in a short time. The final Zn//MnO_2 MB exhibited excellent electrochemical performance with a peak volumetric energy density of 71.3 μWh cm^{-2} $μm^{-1}$ and a power density of 1621.4 μWh cm^{-2} $μm^{-1}$. Wearable Co-Zn alkaline MBs using porous N-coated textile and $Co(OH)_2$@NiCo layered double hydroxide electrodes were also manufactured using the laser scribing technique[29]. Moreover, the laser shone on the electrode material can convert insulating polymers into highly conductive electrode materials, of which laser-reduced graphene oxide is a representative example[30].

In short, laser engraving presents the advantages of high spatial precision and manufacturing efficiency, thereby illustrating its potential to produce MBs at a large scale and low cost. In addition, it can also be used for various materials with high universality. Nevertheless, the laser machines are expensive and the heat effect from the laser can destroy the active materials.

Plasma etching

Plasma etching has been widely used in the field of integrated circuits since the 1980s[23]. Plasma is a type of high-energy ionized gas generated from the collision between gas molecules and high-energy electrons or photons. In contrast to photolithography and laser engraving, plasma cannot directly etch materials into interdigital patterns, but serves as the final auxiliary procedure to remove the excess portions. For the study of MBs, plasma etching is mainly applied to create interstices between anode and cathode electrodes for

electrolyte filling and to produce porous electrodes from non-uniform plasma-sensitive precursors. The thickness of the microelectrodes for plasma treatment should not be too thick to exceed the instrument conditions.

Pikul *et al.* reported a Li-ion MB with high power densities of up to 7.4 mW cm^{-2} μm^{-1} by combining the oxygen plasma etching and electrodeposition techniques[31]. In particular, the polystyrene template self-assembled on a Au current collector was removed by plasma to leave a bicontinuous nickel scaffold with interconnected pores [Figure 3C]. The interdigitated highly porous metallic scaffold offered platforms for the electrodeposition of active materials, namely, NiSn as the anode and MnO_2 as the cathode. This microarchitecture provided large volumes for active material loading while maintaining short ion and electron transport pathways, leading to outstanding rate performance for the Li-ion MB.

Printing techniques

Printing techniques can be categorized as mask-based printing (i.e., screen, offset and spray printing) and direct-ink-writing printing (i.e., inject and 3D printing)[32]. Mask-based printing offers advantages in large-scale and high-throughput fabrication but suffers from the challenges of limited resolution and few predesigned masks. Direct-ink-writing printing involves directly depositing active material inks on a substrate in noncontact and additive manners. Thus, this technique can effectively construct complex structures without sacrificing the dimensional resolution in confined areas. In this section, we survey the three most representative printing techniques, namely, screen printing, inject printing, and 3D printing, for microelectrode fabrication.

Screen printing

Screen printing involves squeezing a sticky ink containing electrode materials, binder, and conductive additives onto the substrates through a predesigned mask with an ink-blocking stencil to obtain desirable microelectrodes[33]. Compared with other printing techniques, screen printing possesses the merits of low footprint production costs, large scalability, and highly efficient operability, endowing it with wide applications in the fabrication of organic solar cells, light emitting devices, and interdigital circuits[22]. Remarkably, it is also feasible to screen print inks on soft substrates, such as paper and cloth, thus signifying its compatibility with wearable MB fabrication[34]. A representative example of the screen printing of a MB was reported by Kumar *et al.*, who fabricated an all-printed Zn-Ag_2O battery[35]. The inks were prepared by mixing a polystyrene-block-polyisoprene-block-polystyrene (SIS) binder and a Zn- or Ag_2O-based slurry. A semi-automatic screen printer was then employed to directly fabricate the Zn-Ag_2O MB [Figure 3D]. Compared with other elastomers, e.g., exoflex, the SIS showed simpler processing and higher elasticity and compatibility with high loading active materials. This all-printed solid-state MB demonstrated an excellent charging/discharging capacity density of 2.5 mAh cm^{-2} after multiple complete stretching cycles. A fully stretchable LIB was also fabricated using screen printing with all printable components, including electrodes, current collectors, separators, and encapsulates[36]. The diverse processability was enabled by a physically cross-linked organogel as the stretchable binder. Despite the attractiveness of screen printing for stretchable MB fabrication, it is not trivial to explore functional binders and processable inks[34]. Moreover, the predesigned patterning mask and the large line width of the stencil are unappealing for manufacturing ultrafine microelectrodes.

Inkjet printing

Inkjet printing is a digital printing technique that can create versatile and precise patterns following programmable digital files[37] without using the predesigned masks featured in screen printing. The printing process can be described as the continuous extrusion of filaments (i.e., colloidal suspensions, hydrogels and

polymers) on various substrates (i.e., metal foil, glass, plastics and papers) to form sophisticated architectures. Another advantage of inkjet printing is the high resolution through the narrow inkjet nozzles. However, inkjet printing suffers from the drawbacks of low-yield and long-time production[38].

A sulfur microelectrode was inkjet-printed for integrated stand-alone microelectronics[39]. The printing ink was prepared by dispersing a desirable amount of sulfur-infused single-wall carbon nanotubes in a cyclohexylpyrrolidone solvent, followed by printing on an Al foil substrate or Pt-coated silicon wafers. Profilometry revealed that the printed sulfur cathode was less than 10 μm in thickness, thus offering a promising platform for flexible and thin-film Li-S MBs. Inject-printed thin-film Si anodes were also fabricated for LIBs using a conductive polymer poly(3,4-ethylenediox-ythiophene)-poly(styrene sulfonate) (PEDOT:PSS) binder and Si nanoparticle active materials [Figure 3E][40]. The PEDOT:PSS could alleviate the huge volume variations of Si nanoparticles during lithiation and delithiation cycles. This favorable property was lacking in other printed Si electrodes utilizing carboxymethyl cellulose, polyvinylidene fluoride, and Na-alginate binders. This work indicated the importance of polymer selection for ink preparation during inkjet printing. A water-soluble $LiFePO_4$ cathode for LIBs was also printed. When comparing the electrochemical performance of the printed cathodes using Al foil and CNT micropaper current collectors, the latter demonstrated higher cyclic capacities, possibly arising from the interaction between the printed active materials and substrates[41].

Overall, the highly accurate and versatile inject printing technique is an excellent choice for MB fabrication. Nevertheless, it still suffers from several limitations, for example, the jamming of nozzles in highly viscous ink, the lower resolution than that of photolithography, and the difficulties in designing inks with process-customized rheology and good dispersion.

3D printing

3D printing, as an advanced additive manufacturing technology, has been widely used to fabricate electrochemical energy storage devices from the nanoscale to the macroscale[21]. In a typical 3D printing process, the printable inks containing the electrode materials are directly printed on current collectors according to the predetermined electrode architectures as programmed in shape, size, and dimensions, and finally packaged with or without an electrolyte filling[42]. Due to its introduction of the third dimension (i.e., height), 3D printing can dramatically enhance the design freedom for any desired shapes, leading to high areal and volumetric energy densities. In addition, through the layer-by-layer plating process, 3D printing can significantly improve the fabrication efficiency and reduce material wastage, potentially saving MB production time by eliminating the assembly steps[8]. Overall, 3D printing opens a new avenue towards precisely manipulating microelectrodes with desirable architectures and performance.

3D printing has been widely applied in the fabrication of monovalent Li-based MBs[43] and multivalent Zn- and Al-based MBs[44,45]. For example, Lacey and co-workers[46] pioneered the printing of a 3D holey graphene oxide (HGO) cathode for lithium-oxygen (Li-O_2) batteries. The holey graphene powder was directly dissolved in water as the printable ink, followed by extrusion-based 3D printing to create hierarchically porous structures layer by layer [Figure 3F]. The 3D printed HGO cathode demonstrated trimodal porosity, from the nanoscale (4-25 nm through holes in HGO) to the macroscale (micrometer-sized pores between the HGO sheets and printed walls), which was beneficial for promoting the fully active sites and the mass-electron transport kinetics, thus dramatically enhancing the overall Li-O_2 battery performance. Kim *et al.* packaged an aqueous Zn-ion MB consisting of a laser micromachined zinc metal anode and a 3D printed polyaniline-coated carbon fiber cathode[44]. The combination of 3D printing, laser micromachining, and electrospinning techniques achieved the arbitrary motifs. The packed Zn-ion MB (~0.3 cm^3) exhibited

outstanding electrochemical performance with a discharge capacity of 162 mAh g^{-1} and 15% capacity fade after 100 cycles. As a prototype demonstration, the Zn-ion MB was integrated with a wearable photosensor, which successfully turned on red LEDs when the cell detected a certain level of darkness. Moreover, representative electrodes, such as $LiFePO_4$ for LIBs[47], $Na_3V_2(PO_4)_2$ for Na-ion batteries[48], and sulfur/carbon composites for Li-S batteries[49], have also been successfully 3D printed.

In summary, 3D printing is an innovative technology that can disruptively change the design and fabrication routes at the levels of electrodes, MBs, and microdevices, arising from its outstanding fabrication and design flexibilities. However, it is noteworthy that the post-thermal treatment of 3D printed electrodes may induce deformation or structural collapse. In addition, the printability is closely related to the ink chemistry. An in-depth and comprehensive understanding of ink chemistry should be elucidated in future studies. Additionally, some newly emerging methods, such as electro-hydrodynamic jet printing[50], holographic lithography[51] and, focused ion beam technology[52], have also been developed to construct high-resolution and high-loading microelectrodes.

STRUCTURAL DESIGN FOR MICROBATTERIES: FROM 2D TO 3D ASSEMBLY

From the above survey of the miniaturization techniques, 2D thin-film (i.e., using photolithography, screen printing process) and 3D framework (i.e., using 3D printing process) are the two major microelectrode architectures. Thin-film electrodes are viable for 2D stacked MBs and bulky batteries, whereas 3D electrodes offer the possibility to build sandwich-type, in-plane type, and concentric-tube-type 3D MBs. Although both MBs architectures retain strength and challenges in terms of fabrication efficiency, battery performance, and assembling capability, a consensus is approaching that 3D structures outperform their 2D counterparts to meet the high energy/power demands.

The first 2D thin-film Li-ion MB was proposed by Kanehori *et al.* in 1983[53]. Since then, a large family of electrode materials and other components (i.e., electrolytes and separators) have been explored. As a well-established configuration, 2D MBs exhibit the notable features of facile design and excellent compatibility with existing industrial manufacturing lines, manifesting its feasibility for large-scale applications. For Li-ion MBs, an initial work was reported by Nakano *et al.*[54], who successfully fabricated a 2D interdigital MB using a sol-gel method [Figure 4A]. $LiMn_2O_4$ and $Li_{4/3}Ti_{5/3}O_4$ (LTO) thin films were used as the cathode and anode materials in the Li-ion MB, respectively. Electrochemical measurements showed that the MB exhibited an operating voltage of 2.45 V and an energy density of 8.48 μWh cm^{-2}. Despite the unfavorable energy density and cyclability, this work demonstrated the feasibility of Li-ion MBs. A fully bendable 2D thin-film LIB was later demonstrated by stacking Li-metal anodes and $LiCoO_2$ cathodes with a lithium phosphorus oxynitride electrolyte (LiPON) in between [Figure 4B][55]. The cm-scale LIB exhibited remarkable electrochemical performance with a high charging voltage of 4.2 V and an energy density of 2.2×10^3 μWh cm^{-2} at 46.5 μA cm^{-2} for 100 cycles [Figure 4C and D]. Flexible LIBs possess significant potential for powering implantable and wearable electronic devices. To improve the energy densities of layered-type MBs, a promising design was constructed for anode-free cells. Without the thick Li metal, the $LiCoO_2$//LiPON//Cu MB delivered a 60% higher energy density than that of common Li-ion MBs, corresponding to a footprint capacity of 0.89 mAh cm^{-2}[56]. However, anode-free LIBs are inclined to lose capacity rapidly due to the continuous Li consumption on both the anode and cathode surfaces.

Despite the encouraging achievements regarding 2D MBs, their limited areal capacities in the range of 0.5 mAh cm^{-2} hinder their practical applications, especially as integrated power sources. In 2D MBs, the energy and power densities are strongly coupled so that it is impossible to concurrently improve both parameters in the limited area. The energy density can be enlarged by making thick-film electrodes, but

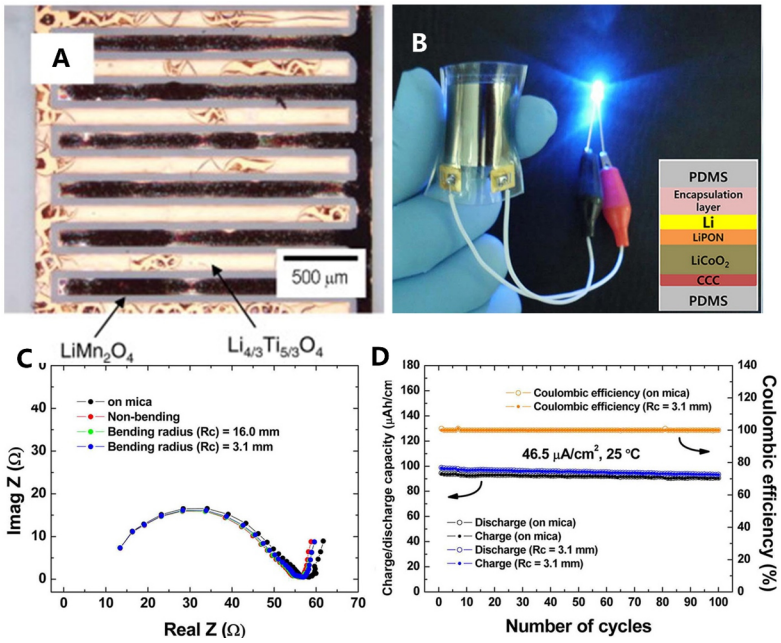

Figure 4. (A) Microscopic image of a 2D interdigital MB (reproduced with permission[54]. Copyright 2007, Elsevier). (B) Photograph of a bendable 2D thin-film MB that could light a blue LED when bent. The inset image shows the layer components of the MB. (C) Nyquist plots of AC impedance test for the bendable 2D MB. (D) Capacity and Coulombic efficiency of the bendable MB over 100 cycles (reproduced with permission[55]. Copyright 2012, ACS Publications). MB: Microbattery.

these would suppress the power density by elongating and twisting the ion/electron transport pathways, as well as damaging the electrode integrity with an inhomogeneous current distribution[57,58]. Detachment of electrode materials from current collectors also occurs in thick-film electrodes. In order to mitigate these issues, 3D microelectrodes that enable the energy and power density requirements to be decoupled have been proposed. As mentioned above, 3D microelectrodes and MBs possess the following advantages: (i) higher power density due to the shorter charge transfer distance in 3D structures; (ii) enhanced mass loading and electrolyte percolation by introducing "the third dimension", leading to high-energy-density MBs; (iii) longer cycle life by eliminating inhomogeneous current distribution and accommodating the volume expansion with adjacent voids; (iv) higher design flexibility and relatively lower manufacturing costs for built-in configurations. A brief development timeline for the upgrading of miniaturization technologies for 3D MBs is displayed in Figure 5.

Among the various 3D MBs, the interdigitated structure is the most representative with high aspect ratios for high active material loadings[59]. Interdigital MBs are composed of two parallel finger-shaped microelectrodes without separators between them[14,60]. Not only does this decrease the overall cell mass by eliminating separators, but the 3D MBs can also be directly built in microelectronics. Sun and co-workers[61] produced a novel 3D interdigital Li-ion MB (denoted as 3D-IMB) using 3D printing. $LiFePO_4$ (LFP) and LTO with negligible volumetric changes during cycling were selected as the cathode and anode materials, respectively, thereby reducing the requirements on structural compliance to accommodate electrode strains. As shown in Figure 6A, the 3D-IMB composed of printed LFP and LTO layers showed dimensions of 960 μm × 800 μm in area and 480 μm in height. The MB exhibited the electrochemical performance of an area capacity of 1.5 mAh cm^{-2} at an operating voltage of 1.8 V and moderate capacity degradation for 30 cycles [Figure 6B and C]. The appreciable stability was attributed to the low-strain topotactic reaction of the active materials. A packaged 3D-IMB was further fabricated to present an area energy density of 9.7 J cm^{-2} at a power density of 2.7 mW cm^{-2}.

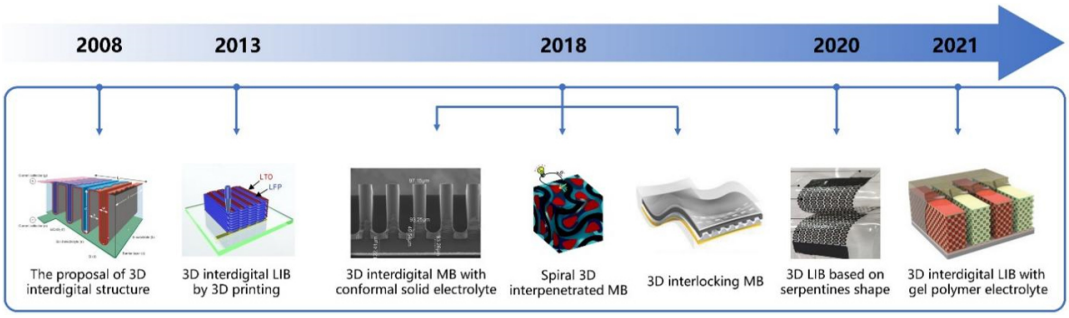

Figure 5. Brief development timeline of representative 3D MBs. Proposal of 3D interdigital structure (reproduced with permission[59]. Copyright 2008, Wiley-VCH). 3D interdigital LIB from 3D printing (reproduced with permission[61]. Copyright 2013, Wiley-VCH). 3D interdigital MB with conformal solid electrolyte (reproduced with permission[26]. Copyright 2018, Elsevier). Spiral 3D interpenetrated MB (reproduced with permission[73]. Copyright 2018, Royal Society of Chemistry). 3D interlocking MB (reproduced with permission[76]. Copyright 2018, Wiley-VCH). 3D LIB based on a serpentine configuration (reproduced with permission[83]. Copyright 2020, Elsevier). 3D interdigital LIB with gel polymer electrolyte (reproduced with permission[70]. Copyright 2021, Wiley-VCH). MBs: Microbatteries; LIB: lithium-ion battery.

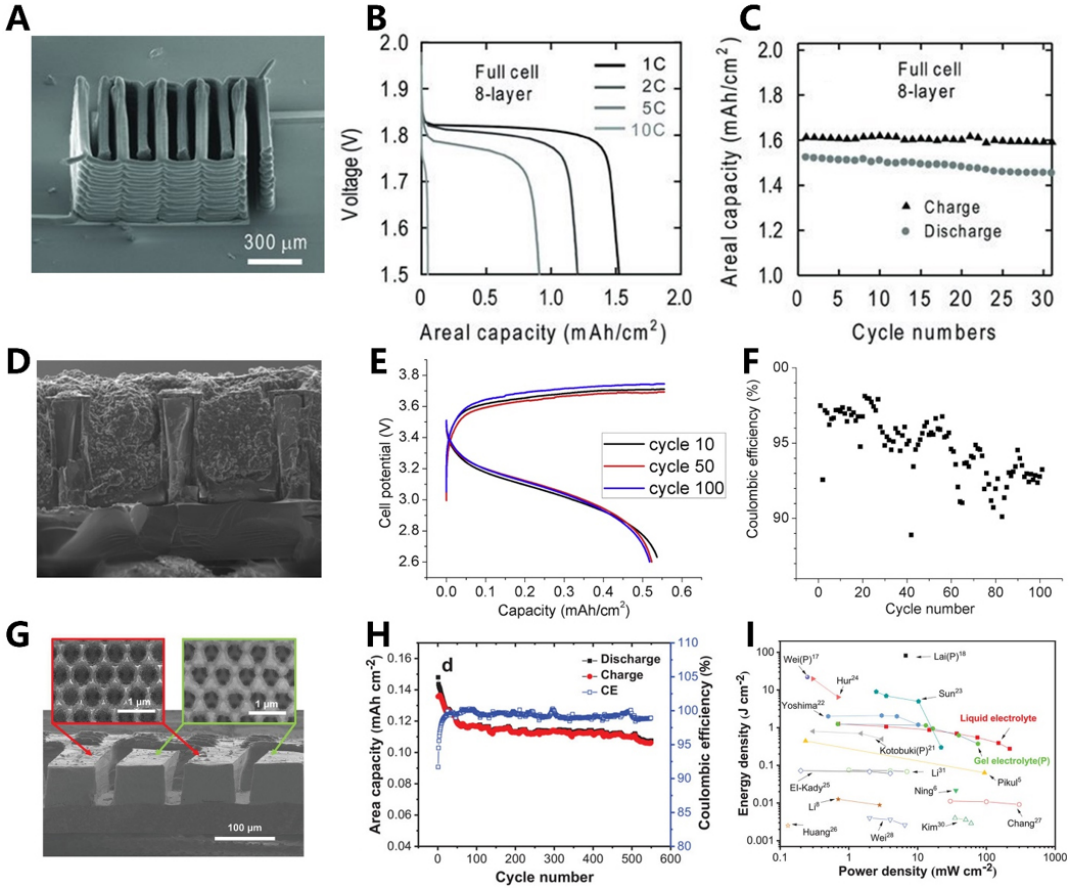

Figure 6. (A) SEM image of printed 3D interdigitated electrodes. (B) Voltage as a function of areal capacity for 3D interdigitated MB. (C) Areal capacity of interdigitated MB within 30 cycles (reproduced with permission[61]. Copyright 2013, Wiley-VCH). (D) SEM image of full 3D interdigitated MB. (E) Cyclic performance of a powerful 3D interdigitated MB. (F) Coulombic efficiency for powerful 3D interdigitated MB over 100 cycles (reproduced with permission[26]. Copyright 2018, Elsevier). (G) Cross-section SEM image of interdigitated MB. (H) Cycling performance of GPE-based 3D interdigitated MB. (I) Ragone plot showing the performance comparison between the GPE-based 3D interdigitated MB and other reported MBs (reproduced with permission[70]. Copyright 2021,Wiley-VCH). SEM: Scanning electron microscopy; MB: microbattery.

In order to further improve the energy density of 3D Li-ion MBs, high-capacity anodes, such as Si and Li metal, have been coupled with high-voltage cathodes. Si is a well-known anode with an extremely high capacity of 4200 mAh g^{-1}; however, a key challenge in realizing such a high capacity is the huge volume expansion (300%) and pulverization of Si materials[62]. Hur *et al.* reported a 3D MB based on SU-8-coated Si arrays by reactive ion etching Si arrays and photopatterning an SU-8-based solid electrolyte[26]. NCA was filled between SU-8-coated Si arrays to form a Li-ion full cell. The scanning electron microscopy (SEM) image of the 3D interdigitated MB is shown in Figure 6D. The small footprint (0.09 cm^2) Li-ion MB [Figure 6E and F] presented an initial discharge capacity of 5.2 mWh cm^{-2} and a reversible capacity of 1.6 mWh cm^{-2} after 100 cycles with an average Coulombic efficiency of above 92%. Similarly, laser-patterned Si/TiN/Ge[63], self-standing porous Si films[64], plasma-etched Si/TiN/Sb nanorod arrays[65], and dry etching Si towers[66] have also been reported for high-energy Li-ion MBs by accommodating the volume expansion of Si materials.

Studies have also been conducted for 3D Li-metal anodes with a high capacity of 3860 mAh g^{-1}. 3D porous architectures (e.g., N-doped carbon[67], cellulose nanofiber gel[68] and MXene array frameworks[69]) were fabricated to mitigate Li dendrite formation and the large volume changes. For example, Sun *et al.* fabricated a 3D-IMB with an ultrahigh power density via imprint lithography and electrodeposition processes[70]. The 3D-IMB consisted of a Li-metal anode, a V_2O_5 cathode, and a LiTFSI-based gel polymer electrolyte [Figure 6G]. The usage of the gel polymer electrolyte and Norland Optical Adhesive package eliminated electrolyte leakage, as commonly occurs in MBs filled with liquid electrolytes. The packed Li metal//gel electrolyte//V_2O_5 MB retained Coulombic efficiencies of ~99% and a decent capacity retention of 75% after 550 cycles [Figure 6H]. Moreover, the 3D-IMB was capable of cycling at 100 C (referring to 3.6 s per charge), rendering an ultrahigh power density of 75.5 mW cm^{-2} [Figure 6I].

The electrolyte is another key component of 3D-IMBs. Sol-gel and polymer electrolytes are the most fabricated due to the easy adjustment of the rheology of inks to meet conformal coating or printing conditions with desirable ionic conductivity, mechanical stability, and thermal properties without electrolyte leakage during cycling[71,72]. For instance, a solid electrolyte made from an SU-8 photoresist was prepared for a full 3D interdigitated MB[26]. The results showed that the 3D microelectrodes could be capable of allowing the ions to transport through the interdigitated structure at a 400 μm thickness. In addition, the ionic conductivity of this conformal solid electrolyte could reach 2.8×10^{-7} S cm^{-1}. Although this value is relatively lower than for liquid electrolytes, it is considered a practical choice for MB fabrication and could guarantee the safe, stable, and long-term operation of the 3D-IMB. In short, solid polymer electrolytes hold great promise for the further development of 3D MBs.

In addition to 3D interdigitated MBs, other 3D MB structures have also shown promise in storing large amounts of charge per footprint area. For example, Werner *et al.* developed a spiral structure with phase dimensions below 20 nm[73]. The nano-3D structure was prepared by assembling the spiral mesoporous carbon anode (black part), polymer electrolyte (blue part), and composite cathode (red part) consisting of sulfur and poly(3,4-ethylene dioxythiophene) [Figure 7A]. The 3D interpenetrated MB demonstrated a stable open-circuit voltage and a discharge plateau at ~2.7 V with a reversible capacity of 0.2 mAh cm^{-2} [Figure 7B and C]. By folding all the nanoscale components into the interpenetrating networks with a high surface area, such a co-continuous 3D gyroidal structure offered structurally robust MBs[74]. Mesoscale Swiss roll is another intriguing structure for achieving high footprint capacities. A prototype Swiss-roll MB was assembled by coupling a Zn anode and an Ag cathode in alkaline electrolytes[75]. The discharge/charge profiles of the Swiss roll retained a 91% capacity as the current density increased from 3 to 7 mA cm^{-2}, implying an excellent rate capability. It is noteworthy that it is difficult to mass fabricate Swiss-roll MBs

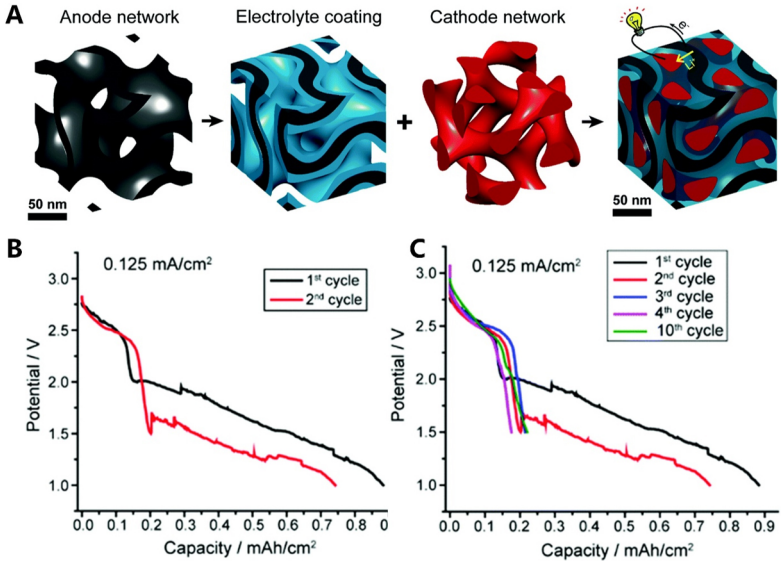

Figure 7. (A) Schematic illustration of preparation pathway of 3D interpenetrated MB. (B) First two cycle performance with the lower cut-off potential at 1 V. (C) Selected cycle performance at 0.125 mA cm^{-2}(reproduced with permission[73].Copyright 2018, Royal Society of Chemistry). MB: Microbattery.

because winding thin and brittle electrode/electrolyte layers either causes shortcuts among layers or lacks mature tools for reproducible production.

Flexible and stretchable MBs play an important role in powering wearable and conformal electronics. To obtain deformable MBs, efforts have been dedicated to (i) synthesizing intrinsically deformable electrodes and electrolytes; (ii) designing specific architectures that can withstand large mechanical changes. A representative example for strategy; (i) is the stretchable 3D-interlocking Li-ion MB [Figure 8A][76]. A graphite anode and $LiCoO_2$ cathode were oppositely patterned. The adhesion forces of both patterned electrodes were two to three times higher than those of conventional thin-film electrodes. When the 3D anode, cathode, and separators were interlocked in a MB, it showed excellent mechanical stability and exhibited a negligible capacity loss in discharging capacity after 5000 flexing cycles [Figure 8B and C], significantly superior to traditional thin-film cells. Similarly, Li-ion MBs based on sponge LTO (anode)/LFP (cathode)[77], Na-ion MBs using stretchable $VOPO_4$ (cathode)/PDMS-rGO (anode)[78] and Li-ion MBs with microhoneycomb G-CNT electrodes[79] have also been reported as stretchable MBs with deformable cell components.

For strategy (ii), wave[80], kirigami[81], zig-zag and serpentine[82] configurations have been proposed for flexible MBs. For example, Nasreldin *et al.* reported a flexible Li-ion MB with vertical electrode micropillars supported on metallic serpentines [Figure 9A][83]. Compared with conventional thin-film MBs, the special architecture revealed advantages in covering a large proportion of substrate area with active materials (> 70%), leaving narrow spaces among electrodes to accommodate the volume change during cycling and improving the power density by amplifying the electrolyte/electrode interface. The 3D Li-ion MB maintained 80% of the initial capacity when a 30% strain was applied to it, while the 2D MB failed under 10% strain. It was also observed that the area capacity for the 3D Li-ion MB was nearly 2.5 times higher than its 2D counterpart [Figure 9B]. To demonstrate the robustness of the stretchable MB, it was cycled under repeated stretching and relaxation for 150 cycles at 1C [Figure 9C], which exhibited a marginal capacity fluctuation even under 30% strain.

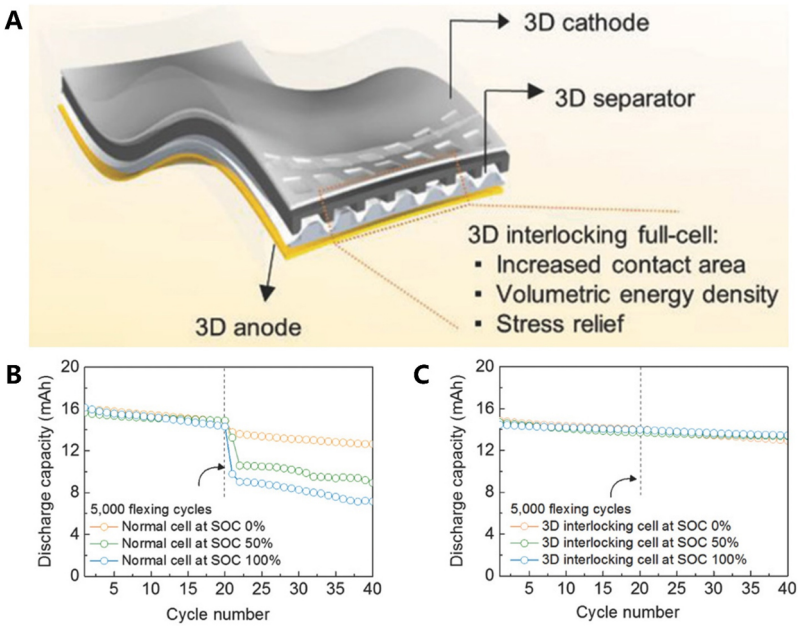

Figure 8. (A) Schematic illustration of 3D interlocking MB. (B) Cycle performance of normal MB at SOC 0%, 50% and 100% over 5000 flexing cycles. (C) Cycle performance of 3D interlocking MB at SOC 0%, 50%, and 100% over 5000 flexing cycles (reproduced with permission[76]. Copyright 2018, Wiley-VCH). MB: Microbattery.

Table 1 summarizes the representative 2D and 3D Li-ion MBs and electrodes reported so far in terms of electrode materials, structures, energy and power densities, and cycle life. It is clear that 3D architecture MBs guarantee both higher energy and power densities than their 2D counterparts by eliminating the trade-off requirements between attainable energy and power for 2D film electrodes. It can also be concluded that the 3D architecture is conducive to the synergistic performance improvement regarding the cyclic stability and rate capability of MBs. Despite the encouraging progress demonstrated, key challenges, including the complex fabrication process, non-scalable production, and poor understanding of ink design, must be overcome before a successful translation of MBs from the lab to market.

POST-LITHIUM MICROBATTERIES

Several fundamental concerns have appeared for LIBs. On the one hand, the concentration of lithium in the Earth's crust is extremely low (< 20 ppm) and unevenly distributed[84]. With the expansion of the energy supply market, the price of Li_2CO_3 (a major raw material for lithium) is surging. On the other hand, the upgrading of microelectronics results in higher requirements regarding volumetric energy density and safety for the energy supply, and it is difficult for Li-based MBs to meet these needs due to the relatively low volumetric capacity and the high activity of lithium metal. To this end, efforts have been devoted to investigating "post-lithium" systems based on sodium, zinc, and aluminum as a result of their high abundance, low price, and good safety[85,86].

Sodium-based MBs employ sodium-ion charge carriers and share a similar cell configuration and charge storage mechanisms as lithium-based MBs[87,88]. Sodium is ubiquitously stored in the Earth's crust and seawater, thus signifying the sustainability and affordability of sodium-based MBs. Although sodium ions exhibit a larger size and higher reduction potential than their lithium counterparts, the comparable volumetric capacity of sodium metal (2046 mAh cm^{-3}) and the feasibility of high voltage cathodes suggest sodium-based MBs are promising for sustainable applications[89]. Furthermore, the larger ionic radius of

Table 1. Summary of different MBs based on their structure and electrochemical performance

Structure	Cathode	Anode	Electrolyte	Capacity	Energy density	Power density	Cycle number	Ref.
2D MB	LMO	LTO	$LiClO_4$/MES polymer	-	8.48 μWh cm^{-2}	-	3	[54]
2D MB	LCO	Li metal	LiPON	106 μAh cm^{-2}	2.2 × 10^3 μWh cm^{-2}	-	100 (98.4%)	[55]
3D interdigital MB	LFP	LTO	$LiClO_4$/EC/DMC	1.5 mAh cm^{-2}	9.7 J cm^{-2}	2.7 mW cm^{-2}	30 (96%)	[61]
3D interdigital MB	$LiNi_{0.8}Co_{0.15}Al_{0.05}O_2$	Lithiated Si	$LiClO_4$/PC	1.8 mAh cm^{-2}	5.2 μWh cm^{-2}	-	100 (92%)	[26]
3D interdigital MB	V_2O_5	Li metal	PEO/LiTFSI/DOL/DME	-	1.24 J cm^{-2}	75.5 mW cm^{-2}	200 (75%)	[70]
3D interpenetrated	S/PEDOT	carbon	PPO	0.2 mAh cm^{-2}	-	-	20	[73]
3D interlocking MB	LCO	graphite	$LiPF_6$/EC/EMC/DMC/VC	-	350 Wh L^{-1}	-	200	[76]
3D MB in serpentines	LNMO	LTO	LiTFSI/MA-PEG500	2.5 mAh cm^{-2}	6.27 mWh cm^{-2}	-	100 (73%)	[83]
3D on-chip MB	LMO	NiSn	$LiClO_4$/EC/DEC	-	6.5 μWh cm^{-2}·$μm^{-1}$	3.6 × 104 μW cm^{-2}	200 (88%)	[51]
3D on-chip MB	LCO	LTO	$LiPF_6$/EC/PC/ETPTA/Al_2O_3	125 mAh g^{-1}	-	-	30 (98%)	[103]
3D on-chip MB	LCO	LTO	$LiPF_6$/EC/PC/ETPTA/Al_2O_3	-	-	1000 WL^{-1}	100 (98%)	[107]
1D flexible MB	MWCNTs/ MnO_2	Li wire	LB303	174.4 mAh g^{-1}	92.84 mWh cm^{-3}	3.9 Wcm^{-3}	-	[109]
1D flexible MB	LFP	LTO	$LiPF_6$ /PVDF- HFP	110 mAh g^{-1}	-	-	30 (81%)	[110]
2D flexible MB	LCO	LTO	$LiPF_6$/EC/DEC	147 mAh g^{-1}	108 mW g^{-1}	-	300 (95%)	[111]
2D flexible MB	LFP	LTO	ionogel	-	146 mW h cm^{-3}	8.8 Wcm^{-3}	3300	[112]
3D flexible MB	LFP	LTO	$LiPF_6$/EC/DEC	-	1.87 mWh cm^{-2}	-	300 (70%)	[77]
3D flexible MB	$VOPO_4$	Hard carbon	$NaClO_4$/PVDF-HFP	103 mA h g^{-1}	1.56 mWh cm^{-2}	-	100 (89%)	[78]
3D flexible MB	LFP	LTO	$LiPF_6$/EC/DEC/DMC	154 mAh g^{-1}	9.18 mWh cm^{-2}	-	100 (95.7%)	[79]

MB: Microbattery.

sodium induces weaker solvation energy within polar solvents. Therefore, sodium-ion electrolytes present high ionic conductivities for high-power sodium-based MBs[90]. For example, a $NaBF_4$-based ionogel electrolyte with robust ionic conductivity of 8.1 mS cm^{-1} was prepared for a quasi-solid-state planar Na-ion MB, which presented a high rate performance with 15.7 mAh cm^{-3} at 30 C and a remarkable areal power density of 55.6 mWh cm^{-3}[91].

Zinc and aluminum metals are far more stable and abundant than lithium. Multivalent ion battery systems have the potential to double (for zinc) or even triple (for aluminum) the capacity of present cathodes, assuming the same amount of charge carriers are inserted[92-94]. In addition, zinc and aluminum metals present overwhelmingly larger volumetric capacities (5854 mA h cm^{-3} for zinc and 8045 mA h cm^{-3} for aluminum) and richer abundance in the Earth's crust (70 ppm for zinc and 8.23% for aluminum) than lithium[85,92]. Moreover, zinc electrodes can work in aqueous electrolytes, thereby simplifying the battery manufacturing condition. Therefore, on-chip[95] and flexible[96,97] Zn-ion MBs have been proposed. For example, Jin *et al.* prepared a flexible Zn-I_2 MB involving I_3^-/I^- redox couples[98]. Compared with other aqueous MBs, this Zn-ion MB could achieve the highest volumetric energy density (1647.3 mWh cm^{-3}) and areal energy

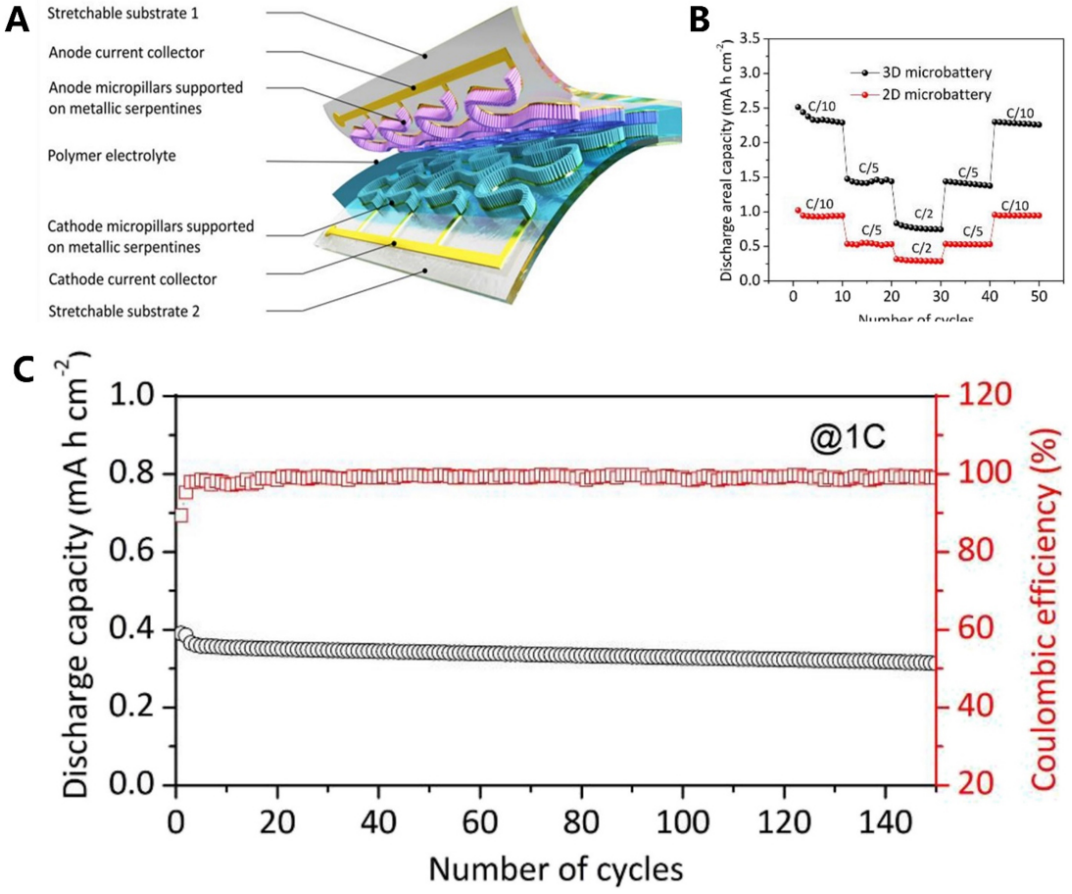

Figure 9. (A) Schematic illustration of 3D flexible MB based on a serpentine configuration. (B) Discharge capacity comparison between 3D and 2D MBs at different C-rates. (C) Discharge capacity and Coulombic efficiency of 3D flexible MB over 150 cycles at 1 C (reproduced with permission[83]. Copyright 2020, Elsevier). MB: Microbattery.

density (2339.1 μWh cm^{-2}). Moreover, this MB also manifested outstanding stability and cyclability with a capacity retention of 89.2% after 2600 cycles. Likewise, Al-based MBs have also attracted significant interest as a result of their high stability for cost-effective energy storage devices. For example, Wang *et al.* fabricated an Al-ion MB based on dual graphite electrodes and an $AlCl_3$/[EMIm]Cl ionic liquid electrolyte[99]. It could offer a high voltage of 2.1 V and a high capacity of 70 mA h g^{-1} after 600 cycles with Coulombic efficiencies above 98%.

Despite the abovementioned advantages for post-lithium systems, there are still a series of challenges that need to be overcome. For example, similar to lithium-based MBs, sodium- and zinc-based MBs also face the problems of dendrite formation and interfacial passivation of the metal anode during cycling. The reduction potential of aluminum [-1.7 V *vs.* standard hydrogen electrode (SHE)] is more positive than lithium (-3.0 V *vs.* SHE), which means that aluminum-based systems are not able to provide competitive cell voltages. In order to solve these problems, studies have been carried out to engineer electrode materials[100,101] and battery structures[102]. We believe that post-lithium MBs could provide new possibilities for next-generation energy storage technologies.

APPLICATION OF MICROBATTERIES

Miniaturized MBs have been increasingly demanded to power stand-alone microelectronics. Here, we present two representative applications of MBs in on-chip integrated microelectronics and wearable devices. In addition to the advance of MB-integrated functional devices, several obstacles related to fabrication fundamentals, electrochemical performance, and adoptability for MBs are also discussed in this section.

MBs for on-chip integration applications

The relentless development of microelectromechanical systems (MEMSs) and complementary metal-oxide-semiconductor-like wireless microsensors and microcomputer requires on-chip integration with miniaturized power sources[95]. For instance, Ning *et al.* designed an on-chip compatible Li-ion MB with high electrochemical performance via a 3D holographic patterning method z[51]. $LiMnO_2$ and NiSn, with high capacities and excellent reversibility, were employed as cathode and anode materials, respectively [Figure 10A]. The packaged MB with dimensions of 10 μm in thickness and 4 mm^2 in area offered an exceptionally high power to light up a red LED after 10 s of charging, which could be cycled 200 times [Figure 10B-D]. Cheong *et al.* reported an organic light-emitting diode-installed pressure sensor powered by a built-in Li-ion MB [Figure 10E][103]. In addition to electrochemical measurements, the self-discharge, thermal stability, and deformable performance of the monolithically integrated Li-ion MB were also studied. The integration of a pressure sensor, smart lens[104], and transparent displays[105] with built-in MBs indicates their significant potential for wireless communication and healthcare applications. Advances in MEMSs have enabled miniaturized computers for autonomous intelligence at the scale of a dust particle. A 0.04-mm^3 computer was recently powered by a built-in Li-ion MB of 1.1 × 1.69 mm^2 area and 150 μm in thickness[106]. This demonstration signifies a future computing platform with autonomous operation.

The integration of various electronic systems in an all-in-one body inevitably results in unwanted energy loss through Joule heat, thus demanding higher energy density for MBs. Apart from boosting the energy per footprint area, the installation of a photovoltaic (PV) panel to construct an energy conversion/storage hybrid system is also promising. For example, a solid-state bipolar Li-ion MB was directly fabricated on a Si PV module through a multistage printing process[107]. The single-unit PV-LIB device (total thickness of 130 μm) exhibited unprecedented improvements in photocharging (less than 2 min charging with a photoelectric conversion efficiency of 7.61%) and photocharge/galvanostatic discharge cycling performance (capacity retention of > 98% after 100 cycles) compared to the Si PVs or Li-ion MB alone.

Despite the progress achieved, several critical problems for built-in MBs in microelectronics remain to be solved, including (i) the insufficient power density of current MBs to meet the demands in reality; (ii) the complex miniaturing process, and thus the high cost of these devices; (iii) the poor compatibility of MBs with components in integrated microsystems for long-term operation[85,108]. To tackle these issues, some possible strategies are recommended, such as the seamless deposition of MBs on microdevices, adjusting the active materials chemistry for all-solid-state MBs and optimizing the monolithic structuring technology.

MBs for wearable device applications

The rapid expansion of wearable electronics, from biomedical devices to smart glasses, has placed increasing research interest in MBs, which hold the promise to realize stand-alone operations. An ideal MB for wearable electronics should satisfy the requirements of mechanical flexibility, clothing breathability, and electrochemical stability. The preferred features for MBs in wearable devices are high energy/power densities and a long lifespan under cyclic deforming. MBs for wearable devices can be categorized on the basis of their dimensions.

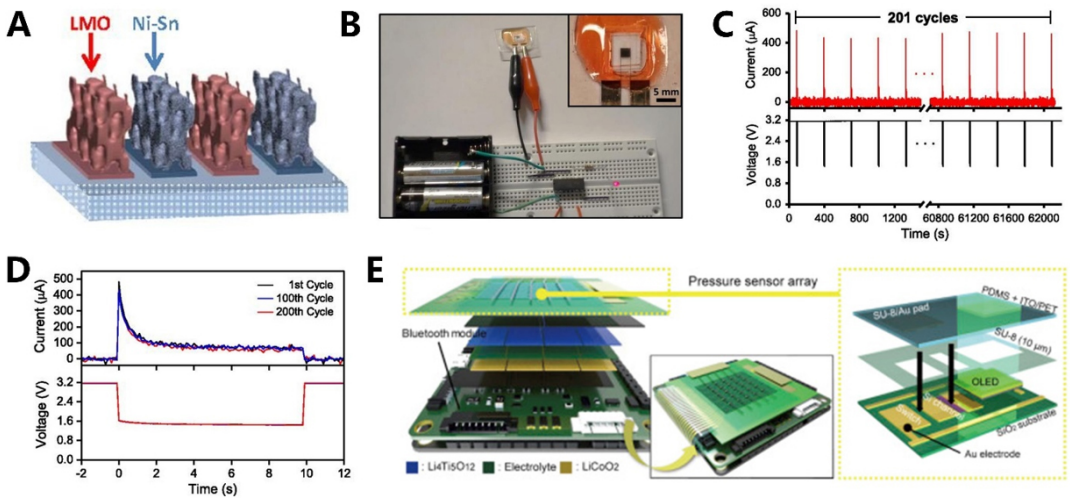

Figure 10. (A) Schematic illustration of an on-chip LMO-NiSn MB. (B) Photograph of on-chip MB connected to a red LED. The inset image shows the on-chip MB. (C) Current and voltage of MB over 201 cycles. (D) Output current and voltage of on-chip MB for the 1st, 100th and 200th cycles (reproduced with permission[51]. Copyright 2015, National Academy of Sciences). (E) Schematic illustration of integrated pressure sensor with on-chip MB (reproduced with permission[103]. Copyright 2019, Elsevier). MB: Microbattery.

The 1D flexible MBs, also known as fiber-shaped MBs, possess strengths regarding electrochemical performance, mechanical flexibility, and straining stability. Fiber-shaped MBs can be categorized as parallel, twisted, coaxial, and coiled structures. Among them, the twisted structure is considered most appealing because of its unique compatibility with the commercial textile industry. For instance, Ren *et al.* proposed a wire-shaped MB by twisting aligned multi-walled carbon nanotubes (MWCNTs) with MnO_2 and lithium wire as the cathode and anode, respectively [Figure 11A][109]. The MnO_2-deposited MWCNT cathode showed improved power density by introducing pseudocapacitance. Subsequently, Wang and co-workers[110] produced an all-fiber-shaped Li-ion MB by twisting 3D printed fibrous electrodes in a gel polymer electrolyte [Figure 11B]. The highly viscous LFP or LTO mixtures with a polymer binder and conducting CNTs were printed into fiber-shaped cathodes and anodes, respectively. PVDF-co-HFP was then coated on the surface of electrode fibers and soaked in electrolytes before being twisted together into integrated fibers. The rheological and electrochemical results showed that the fiber-shaped MB demonstrated strong mechanical strength and excellent full-cell capacities of ~100 mAh g^{-1} after 30 cycles. The fiber-shaped MBs are potential e-textile fabrics for wearable textile applications.

2D paper-like MBs have also received significant attention due to their thin, light, and easy trimming characteristics. For example, Hu *et al.* synthesized a Li-ion MB on paper via a facile lamination method [Figure 11C][111]. The flexible and porous paper was used as the separator and the mechanical substrate. Highly conductive and lightweight CNT films were prepared as the current collector for the positive and negative electrodes on the paper. The ultrathin LCO/LTO paper-like MB (~300 μm) exhibited robust mechanical flexibility (bending down to < 6 mm) and a high energy density (108 mWh g^{-1}). Zheng *et al.* fabricated a flexible planar interdigitating Li-ion MB with a superior volumetric energy density (125.5 mWh cm^{-3}) and long cycling life (3300 times) [Figure 11D][112]. LTO and LFP were chosen as the anode and cathode, respectively. The Li-ion MB was easily fabricated with an ionogel electrolyte by a mask-assisted deposition method. The excellent flexible and electrochemical performance of this planar MB demonstrated its promising industrialization in bendable electronics.

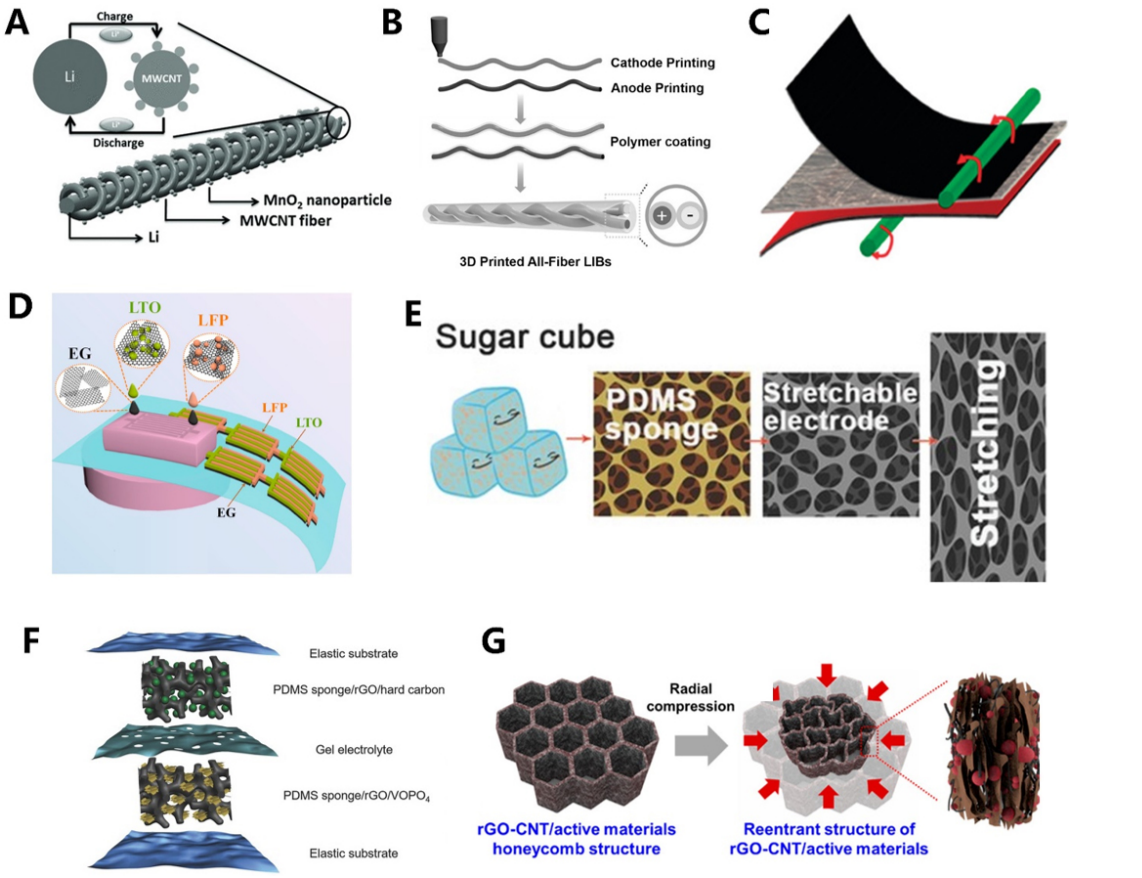

Figure 11. (A) Schematic illustration of a twisted 1D flexible MB (reproduced with permission[109]. Copyright 2013, Wiley-VCH). (B) Schematic illustration of an all-fiber MB based on 3D printing technology (reproduced with permission[110]. Copyright 2017, Wiley-VCH). (C) Schematic illustration of a 2D paper MB (reproduced with permission[111]. Copyright 2010, ACS Publications). (D) Schematic illustration of flexible planar LIMB (reproduced with permission[112]. Copyright 2018, Elsevier). (E) Schematic illustration for the preparation process of a 3D flexible structure (reproduced with permission[77]. Copyright 2016, Wiley-VCH). (F) Schematic illustration of fabricated flexible Na-ion MB (reproduced with permission[78]. Copyright 2017, Wiley-VCH). (G) Honeycomb structure of electrode (reproduced with permission[79]. Copyright 2020, ACS Publications). MB: Microbattery.

3D MBs are always accompanied by porous electrodes. In contrast to 1D and 2D MBs, the 3D framework can achieve higher areal capacity and rate performance. Techniques, such as laser engraving, screen printing, and 3D printing, support the 3D miniaturization fabrication. For example, Liu *et al.* designed a stretchable sponge-like Li-ion MB with interconnected pores [Figure 11E] by using a stretchable polydimethylsiloxane (PDMS) host and surge cubes as a sacrificial template[77]. The 3D porous LTO or LFP electrodes offered an elastic response to a large 80% strain while retaining the stable electrochemical response. Full cells consisting of stretchable LTO and LFP electrodes delivered a high capacity retention after 330 cycles. Nevertheless, the use of liquid electrolytes may cause leakage problems in wearable device applications[113]. To mitigate this issue, Li *et al.* produced a stretchable Na-ion MB based on graphene oxide (rGO)-modified PDMS (PDMS/rGO) sponge scaffold[78]. In this MB [Figure 11F], $VOPO_4$ and hard carbon were integrated into PDMS/rGO as the cathode and anode materials, respectively, which were separated by a PVDF-HFP gel separator/electrolyte. Owing to the high conductivity and mechanical flexibility of PDMS/rGO, the packaged Na-ion MB presented 85% capacity retention after 100 cycles at 1C and 89% of the specific capacity after 100 cycles of stretching to 50% strain. In order to overcome the low energy density caused by the inert PDMS, Kang *et al.* proposed honeycomb-shaped electrodes based on a graphene-CNT composite substrate [Figure 11G][79]. Compared with PDMS, the graphene and CNTs exhibited a larger

surface area, better conductivity, and stronger flexibility, and therefore represent ideal options for stretchable electrode fabrication.

In conclusion, on-chip and flexible MBs can be integrated as power sources for a broad range of microelectronics. The crucial target is to promote the mechanical and thermal stability, portability and compatibility with functional microelectronics. Apart from being utilized as power supplies, MBs could also be used as functional components, like stress sensors[114], and characterization platforms[115] to meet emerging applications. Moreover, the self-healing[116] and self-charging[117] properties of MBs have also been explored for applications in specific scenarios. It is therefore expected that MBs will be useful in a wide range of interests.

SUMMARY AND PERSPECTIVE

In summary, MBs have played a key role in powering wireless and autonomous microelectronics in modern society. In this review, we examined the recent progress in MBs from the perspectives of manufacturing technologies, electrode materials and structures, battery assembly structures, battery performance and applications. To date, advanced fabrication techniques, categorized as etching and printing, have been developed to manufacture various electrode architectures. Moreover, these microelectrodes can be assembled into 2D or 3D MBs, with the latter demonstrating more favorability with simultaneously enhanced energy and power densities. The development of post-lithium MBs and stand-alone microelectronic/wearable devices have also been highlighted. The accumulated knowledge will stimulate the further advancement of MBs to realize true autonomous systems. Despite the tremendous progress in both the manufacturing technologies and performance of MBs, their development is still far behind expectations. Several crucial points are suggested to be overcome in future studies:

(i) *Advanced electrodes and electrolytes.* The performance of MBs highly depends on the properties of the anode/cathode materials and electrolytes. Understanding the material-electrochemical property relationship is of essence to rationalizing the selection and fabrication of MB components. The desirable electrode materials should offer high capacity, fast charge transfer rate, and proper mechanical characteristics to fit the miniaturization processes. Furthermore, novel electrolytes with excellent ionic conductivities and mechanical robustness are desired to eliminate the leakage and inflammation problems of current electrolyte systems. To better understand the insights into the materials of MB architectures, *in-situ* or *operando* characterization techniques to monitor the evolution of cell components in working cells should also be developed.

(ii) *Easily accessible fabrication techniques*. The microstructures of electrodes or MBs play a crucial role in determining the energy/power density and operating stability. Although many techniques have been developed to fabricate various microelectrodes or MBs, the majority of current downsizing approaches are complicated, tedious, and require less-accessible equipment to researchers. In addition, the low-yielding, lab-scale, and less reproducible preparation is far from ready to be transformed to industrial production. Studies in developing low-cost, fast, convenient, and accurate fabrication techniques are imperatively required. To achieve higher energy density in the limited footprint area, lithium-sulfur, lithium-metal, and zinc-metal MBs with much higher theoretical capacities than conversion LIBs have recently been explored. Studies in these emerging systems are still at the beginning and more efforts are required to accelerate the development of these promising electrochemical systems.

(iii) *Optimized integration of MBs with microelectronic systems*. To meet the purpose of developing MBs for stand-alone microelectronics, the role of device packaging cannot be overlooked. The complexity of MB

structures and the manufacturing process induce difficulties in its monolithic integration with microelectronic devices. Some high-end and newly emerging technologies (i.e., artificial intelligence, implantable devices and wireless charging) have rarely been demonstrated to form all-in-one electronics with MBs. Therefore, attention should be paid to establishing smart packaging strategies and microdevice configurations. In this sense, thermal stable solid or gel electrolytes, high energy post-Li batteries, and compatible manufacturing techniques would be favorable. Although progress can be accompanied by regression, it is believed that more efforts in MBs studies will bring us closer to an era of smart microelectronics featuring ubiquitous operations.

DECLARATIONS

Acknowledgments

The work described in this paper was mainly supported by the funding support to the State Key Laboratories in Hong Kong from the Innovation and Technology Commission (ITC) of the Government of the Hong Kong Special Administrative Region (HKSAR), China. The authors would like to express their sincere thanks to the financial support from the Research Office (Project code: 1-BBXK, A-PB1M) of The Hong Kong Polytechnic University.

Authors' contributions

Conceived and designed the manuscript: Chen F, Xu ZL
Drafted and revised the manuscript: Chen F, Xu ZL

Availability of data and materials

Not applicable.

Financial support and sponsorship

The authors would like to express their sincere thanks to the financial support from the Research Office (Project code: 1-BBXK, A-PB1M) of The Hong Kong Polytechnic University.

Conflicts of interest

All authors declared that there are no conflicts of interest.

Ethical approval and consent to participate

Not applicable.

Consent for publication

Not applicable.

REFERENCES

1. Kittner N, Lill F, Kammen DM. Energy storage deployment and innovation for the clean energy transition. *Nat Energy* 2017;2:1-6. DOI
2. Oudenhoven JFM, Baggetto L, Notten PHL. All-solid-state lithium-ion microbatteries: a review of various three-dimensional concepts. *Adv Energy Mater* 2011;1:10-33. DOI
3. Kyerematen NA, Brousse T, Pech D. Microsupercapacitors as miniaturized energy-storage components for on-chip electronics. *Nat Nanotechnol* 2017;12:7-15. DOI PubMed
4. Hong X, Ma X, He L, et al. Regulating lattice-water-adsorbed ions to optimize intercalation potential in 3D prussian blue based multi-ion microbattery. *Small* 2021;17:e2007791. DOI PubMed
5. Pan X, Hong X, Xu L, Li Y, Yan M, Mai L. On-chip micro/nano devices for energy conversion and storage. *Nano Today*

2019;28:100764. DOI
6. Mckelvey K, Brunet Cabré M, Esmeraldo Paiva A. Continuum simulations for microscale 3D batteries. *Curr Opin Electrochem* 2020;21:76-83. DOI
7. Yue C, Li J, Lin L. Fabrication of Si-based three-dimensional microbatteries: a review. *Front Mech Eng* 2017;12:459-76. DOI
8. Yang Y, Yuan W, Zhang X, et al. Overview on the applications of three-dimensional printing for rechargeable lithium-ion batteries. *Appl Energy* 2020;257:114002. DOI
9. Xu B, Qian D, Wang Z, Meng YS. Recent progress in cathode materials research for advanced lithium ion batteries. *Mater Sci Eng R Rep* 2012;73:51-65. DOI
10. Zhang X, Chen Y, Ma F, et al. Regulating Li uniform deposition by lithiophilic interlayer as Li-ion redistributor for highly stable lithium metal batteries. *Chem Eng J* 2022;436:134945. DOI
11. Zhang X, Chen Y, Srinivas K, et al. Lithiophilic Mo_3N_2/MoN as multifunctional interlayer for dendrite-free and ultra-stable lithium metal batteries. *J Colloid Interface Sci* 2022;612:332-41. DOI PubMed
12. Shi Y, Fu J, Hui K, et al. Promoting the electrochemical properties of yolk-shell-structured CeO2 composites for lithium-ion batteries. *Microstructures* 2021;1:2021005. DOI
13. Park S, Jin HJ, Yun YS. Advances in the design of 3D-structured electrode materials for lithium-metal anodes. *Adv Mater* 2020;32:e2002193. DOI PubMed
14. Zhu Z, Kan R, Hu S, et al. Recent advances in high-performance microbatteries: construction, application, and perspective. *Small* 2020;16:e2003251. DOI PubMed
15. Zoller F, Böhm D, Bein T, Fattakhova-Rohlfing D. Tin oxide based nanomaterials and their application as anodes in lithium-ion batteries and beyond. *ChemSusChem* 2019;12:4140-59. DOI PubMed PMC
16. Fang X, Peng H. A revolution in electrodes: recent progress in rechargeable lithium-sulfur batteries. *Small* 2015;11:1488-511. DOI PubMed
17. Pei P, Wang K, Ma Z. Technologies for extending zinc-air battery's cyclelife: A review. *Appl Energy* 2014;128:315-24. DOI
18. Yang H, Li H, Li J, et al. The rechargeable aluminum battery: opportunities and challenges. *Angew Chem Int Ed Engl* 2019;58:11978-96. DOI PubMed
19. Sharifi T, Valvo M, Gracia-espino E, Sandström R, Edström K, Wågberg T. Hierarchical self-assembled structures based on nitrogen-doped carbon nanotubes as advanced negative electrodes for Li-ion batteries and 3D microbatteries. *J Power Sources* 2015;279:581-92. DOI
20. Tang H, Karnaushenko DD, Neu V, et al. Stress-actuated spiral microelectrode for high-performance lithium-ion microbatteries. *Small* 2020;16:e2002410. DOI PubMed
21. Zhang M, Mei H, Chang P, Cheng L. 3D printing of structured electrodes for rechargeable batteries. *J Mater Chem A* 2020;8:10670-94. DOI
22. Liu N, Gao Y. Recent progress in micro-supercapacitors with in-plane interdigital electrode architecture. *Small* 2017;13:1701989. DOI PubMed
23. Duan Y, You G, Sun K, et al. Advances in wearable textile-based micro energy storage devices: structuring, application and perspective. *Nanoscale Adv* 2021;3:6271-93. DOI
24. Wu Z, Parvez K, Feng X, Müllen K. Photolithographic fabrication of high-performance all-solid-state graphene-based planar micro-supercapacitors with different interdigital fingers. *J Mater Chem A* 2014;2:8288. DOI
25. Choi CS, Lau J, Hur J, Smith L, Wang C, Dunn B. Synthesis and properties of a photopatternable lithium-ion conducting solid electrolyte. *Adv Mater* 2018;30:1703772. DOI PubMed
26. Hur JI, Smith LC, Dunn B. High areal energy density 3D lithium-ion microbatteries. *Joule* 2018;2:1187-201. DOI
27. Mamidi S, Kakunuri M, Sharma CS. Fabrication of SU-8 derived three-dimensional carbon microelectrodes as high capacity anodes for lithium-ion batteries. *ECS Trans* 2018;85:21-7. DOI
28. Lai W, Wang Y, Lei Z, et al. High performance, environmentally benign and integratable Zn//MnO_2 microbatteries. *J Mater Chem A* 2018;6:3933-40. DOI
29. Wang Y, Hong X, Guo Y, et al. Wearable Textile-Based Co-Zn alkaline microbattery with high energy density and excellent reliability. *Small* 2020;16:e2000293. DOI PubMed
30. Lobo DE, Banerjee PC, Easton CD, Majumder M. Miniaturized supercapacitors: focused ion beam reduced graphene oxide supercapacitors with enhanced performance metrics. *Adv Energy Mater* 2015;5:1500665. DOI
31. Pikul JH, Gang Zhang H, Cho J, Braun PV, King WP. High-power lithium ion microbatteries from interdigitated three-dimensional bicontinuous nanoporous electrodes. *Nat Commun* 2013;4:1732. DOI PubMed
32. Lee K, Ahn DB, Kim J, Lee J, Lee S. Printed built-in power sources. *Matter* 2020;2:345-59. DOI
33. Costa C, Gonçalves R, Lanceros-méndez S. Recent advances and future challenges in printed batteries. *Energy Storage Mater* 2020;28:216-34. DOI
34. Zhang Y, Zhu Y, Zheng S, et al. Ink formulation, scalable applications and challenging perspectives of screen printing for emerging printed microelectronics. *J Energy Chem* 2021;63:498-513. DOI
35. Kumar R, Shin J, Yin L, You J, Meng YS, Wang J. All-printed, stretchable Zn-Ag_2O rechargeable battery via hyperelastic binder for self-powering wearable electronics. *Adv Energy Mater* 2017;7:1602096. DOI
36. Hong SY, Jee SM, Ko Y, et al. Intrinsically stretchable and printable lithium-ion battery for free-form configuration. *ACS Nano*

2022;16:2271-81. DOI PubMed
37. Nayak L, Mohanty S, Nayak SK, Ramadoss A. A review on inkjet printing of nanoparticle inks for flexible electronics. *J Mater Chem C* 2019;7:8771-95. DOI
38. Choi K, Ahn DB, Lee S. Current status and challenges in printed batteries: toward form factor-free, monolithic integrated power sources. *ACS Energy Lett* 2018;3:220-36. DOI
39. Milroy CA, Jang S, Fujimori T, Dodabalapur A, Manthiram A. Inkjet-printed lithium-sulfur microcathodes for all-printed, integrated nanomanufacturing. *Small* 2017;13:1603786. DOI PubMed
40. Lawes S, Sun Q, Lushington A, Xiao B, Liu Y, Sun X. Inkjet-printed silicon as high performance anodes for Li-ion batteries. *Nano Energy* 2017;36:313-21. DOI
41. Gu Y, Wu A, Sohn H, Nicoletti C, Iqbal Z, Federici JF. Fabrication of rechargeable lithium ion batteries using water-based inkjet printed cathodes. *J Manuf Process* 2015;20:198-205. DOI
42. Ejeian M, Wang R. Adsorption-based atmospheric water harvesting. *Joule* 2021;5:1678-703. DOI
43. Cohen E, Menkin S, Lifshits M, et al. Novel rechargeable 3D-Microbatteries on 3D-printed-polymer substrates: Feasibility study. *Electrochim Acta* 2018;265:690-701. DOI
44. Kim C, Ahn BY, Wei TS, et al. High-power aqueous zinc-ion batteries for customized electronic devices. *ACS Nano* 2018;12:11838-46. DOI PubMed
45. Yu Y, Chen M, Wang S, et al. Laser sintering of printed anodes for al-air batteries. *J Electrochem Soc* 2018;165:A584-92. DOI
46. Lacey SD, Kirsch DJ, Li Y, et al. Extrusion-based 3D printing of hierarchically porous advanced battery electrodes. *Adv Mater* 2018;30:e1705651. DOI PubMed
47. Hu J, Jiang Y, Cui S, et al. 3D-Printed cathodes of $LiMn_1$-xFe_xPO4 nanocrystals achieve both ultrahigh rate and high capacity for advanced lithium-ion battery. *Adv Energy Mater* 2016;6:1600856. DOI
48. Ding J, Shen K, Du Z, Li B, Yang S. 3D-Printed hierarchical porous frameworks for sodium storage. *ACS Appl Mater Interfaces* 2017;9:41871-7. DOI PubMed
49. Cai J, Fan Z, Jin J, et al. Expediting the electrochemical kinetics of 3D-printed sulfur cathodes for Li-S batteries with high rate capability and areal capacity. *Nano Energy* 2020;75:104970. DOI
50. Park JU, Hardy M, Kang SJ, et al. High-resolution electrohydrodynamic jet printing. *Nat Mater* 2007;6:782-9. DOI PubMed
51. Ning H, Pikul JH, Zhang R, et al. Holographic patterning of high-performance on-chip 3D lithium-ion microbatteries. *Proc Natl Acad Sci USA* 2015;112:6573-8. DOI PubMed PMC
52. Zhuang P, Sun Y, Li L, et al. FIB-patterned nano-supercapacitors: minimized size with ultrahigh performances. *Adv Mater* 2020;32:e1908072. DOI PubMed
53. Kanehori K, Matsumoto K, Miyauchi K, Kudo T. Thin film solid electrolyte and its application to secondary lithium cell. *Solid State Ionics* 1983;9-10:1445-8. DOI
54. Nakano H, Dokko K, Sugaya J, Yasukawa T, Matsue T, Kanamura K. All-solid-state micro lithium-ion batteries fabricated by using dry polymer electrolyte with micro-phase separation structure. *Electrochem Commun* 2007;9:2013-7. DOI
55. Koo M, Park KI, Lee SH, et al. Bendable inorganic thin-film battery for fully flexible electronic systems. *Nano Lett* 2012;12:4810-6. DOI PubMed
56. Oukassi S, Bazin A, Secouard C, et al. Millimeter scale thin film batteries for integrated high energy density storage. In 2019 IEEE International Electron Devices Meeting (IEDM); 2019, p.26.1.1-26.1.4. (ISBN No. 2156-017X) DOI
57. Sha M, Zhao H, Lei Y. Updated insights into 3D architecture electrodes for micropower sources. *Adv Mater* 2021;33:e2103304. DOI PubMed
58. Wang J, Shen Z. Modeling-guided understanding microstructure effects in energy storage dielectrics. *Microstructures* 2021;1:2021006. DOI
59. Baggetto L, Niessen RAH, Roozeboom F, Notten PHL. High energy density all-solid-state batteries: a challenging concept towards 3D integration. *Adv Funct Mater* 2008;18:1057-66. DOI
60. Lyu Z, Lim GJ, Koh JJ, et al. Design and manufacture of 3D-printed batteries. *Joule* 2021;5:89-114. DOI
61. Sun K, Wei TS, Ahn BY, Seo JY, Dillon SJ, Lewis JA. 3D printing of interdigitated Li-ion microbattery architectures. *Adv Mater* 2013;25:4539-43. DOI PubMed
62. Xu Z, Liu X, Luo Y, Zhou L, Kim J. Nanosilicon anodes for high performance rechargeable batteries. *Prog Mater Sci* 2017;90:1-44. DOI
63. Yue C, Zhang S, Yu Y, et al. Laser-patterned Si/TiN/Ge anode for stable Si based Li-ion microbatteries. *J Power Sources* 2021;493:229697. DOI
64. Zhao X, Kalidas N, Lehto V. Self-standing mesoporous Si films as anodes for lithium-ion microbatteries. *J Power Sources* 2022;529:231269. DOI
65. Yue C, Wu M, Cheng B, et al. Fabrication of multilayer Si/TiN/Sb NR arrays as anode for 3D Si-based lithium/sodium ion microbatteries. *Adv Mater Interfaces* 2020;7:2001043. DOI
66. Sternad M, Hirtler G, Sorger M, et al. A Lithium-silicon microbattery with anode and housing directly made from semiconductor grade monocrystalline Si. *Adv Mater Technol* 2022;7:2100405. DOI
67. Lyu Z, Lim GJ, Guo R, et al. 3D-printed electrodes for lithium metal batteries with high areal capacity and high-rate capability. *Energy Storage Mater* 2020;24:336-42. DOI

68. Cao D, Xing Y, Tantratian K, et al. 3D Printed High-performance lithium metal microbatteries enabled by nanocellulose. *Adv Mater* 2019;31:e1807313. DOI PubMed
69. Shen K, Li B, Yang S. 3D printing dendrite-free lithium anodes based on the nucleated MXene arrays. *Energy Storage Mater* 2020;24:670-5. DOI
70. Sun P, Li X, Shao J, Braun PV. High-performance packaged 3D lithium-ion microbatteries fabricated using imprint lithography. *Adv Mater* 2021;33:e2006229. DOI PubMed
71. Dudney N. Solid-state thin-film rechargeable batteries. *Mater Sci Eng B* 2005;116:245-9. DOI
72. Cao T, Shi X, Zou J, Chen Z. Advances in conducting polymer-based thermoelectric materials and devices. *Microstructures* 2021;1:2021007. DOI
73. Werner JG, Rodríguez-calero GG, Abruña HD, Wiesner U. Block copolymer derived 3-D interpenetrating multifunctional gyroidal nanohybrids for electrical energy storage. *Energy Environ Sci* 2018;11:1261-70. DOI
74. Ergang NS, Fierke MA, Wang Z, Smyrl WH, Stein A. Fabrication of a fully infiltrated three-dimensional solid-state interpenetrating electrochemical cell. *J Electrochem Soc* 2007;154:A1135. DOI
75. Li Y, Zhu M, Bandari VK, et al. On-Chip batteries for dust-sized computers. *Adv Energy Mater* 2022;12:2270051. DOI
76. Cha H, Lee Y, Kim J, Park M, Cho J. Flexible 3D interlocking lithium-ion batteries. *Adv Energy Mater* 2018;8:1801917. DOI
77. Liu W, Chen Z, Zhou G, et al. 3D porous sponge-inspired electrode for stretchable lithium-ion batteries. *Adv Mater* 2016;28:3578-83. DOI PubMed
78. Li H, Ding Y, Ha H, et al. An all-stretchable-component sodium-ion full battery. *Adv Mater* 2017;29:1700898. DOI PubMed
79. Kang S, Hong SY, Kim N, et al. Stretchable lithium-ion battery based on re-entrant micro-honeycomb electrodes and cross-linked gel electrolyte. *ACS Nano* 2020;14:3660-8. DOI PubMed
80. Liu W, Chen J, Chen Z, et al. Stretchable lithium-ion batteries enabled by device-scaled wavy structure and elastic-sticky separator. *Adv Energy Mater* 2017;7:1701076. DOI
81. Song Z, Wang X, Lv C, et al. Kirigami-based stretchable lithium-ion batteries. *Sci Rep* 2015;5:10988. DOI PubMed PMC
82. Xu S, Zhang Y, Cho J, et al. Stretchable batteries with self-similar serpentine interconnects and integrated wireless recharging systems. *Nat Commun* 2013;4:1543. DOI PubMed
83. Nasreldin M, Delattre R, Calmes C, et al. High performance stretchable Li-ion microbattery. *Energy Storage Mater* 2020;33:108-15. DOI
84. Kubota K, Dahbi M, Hosaka T, Kumakura S, Komaba S. Towards K-Ion and Na-Ion batteries as "Beyond Li-Ion". *Chem Rec* 2018;18:459-79. DOI PubMed
85. Ni J, Dai A, Yuan Y, Li L, Lu J. Three-Dimensional microbatteries beyond lithium ion. *Matter* 2020;2:1366-76. DOI
86. Shi F, Chen C, Xu Z. Recent advances on electrospun nanofiber materials for post-lithium ion batteries. *Adv Fiber Mater* 2021;3:275-301. DOI
87. Yabuuchi N, Kubota K, Dahbi M, Komaba S. Research development on sodium-ion batteries. *Chem Rev* 2014;114:11636-82. DOI PubMed
88. Park J, Xu ZL, Kang K. Solvated ion intercalation in graphite: sodium and beyond. *Front Chem* 2020;8:432. DOI PubMed PMC
89. Xu Z, Park J, Yoon G, Kim H, Kang K. Graphitic carbon materials for advanced sodium-ion batteries. *Small Methods* 2019;3:1800227. DOI
90. Kuratani K, Uemura N, Senoh H, Takeshita H, Kiyobayashi T. Conductivity, viscosity and density of MClO4 (M = Li and Na) dissolved in propylene carbonate and γ-butyrolactone at high concentrations. *J Power Sources* 2013;223:175-82. DOI
91. Zheng S, Huang H, Dong Y, et al. Ionogel-based sodium ion micro-batteries with a 3D Na-ion diffusion mechanism enable ultrahigh rate capability. *Energy Environ Sci* 2020;13:821-9. DOI
92. Muldoon J, Bucur CB, Gregory T. Quest for nonaqueous multivalent secondary batteries: magnesium and beyond. *Chem Rev* 2014;114:11683-720. DOI PubMed
93. Chen C, Shi F, Zhang S, Su Y, Xu ZL. Ultrastable and high energy calcium rechargeable batteries enabled by calcium intercalation in a NASICON cathode. *Small* 2022;18:e2107853. DOI PubMed
94. Chen C, Shi F, Xu Z. Advanced electrode materials for nonaqueous calcium rechargeable batteries. *J Mater Chem A* 2021;9:11908-30. DOI
95. Hao Z, Xu L, Liu Q, et al. On-Chip Ni-Zn microbattery based on hierarchical ordered porous Ni@Ni(OH)$_2$ Microelectrode with ultrafast ion and electron transport kinetics. *Adv Funct Mater* 2019;29:1808470. DOI
96. Bi S, Wan F, Wang S, Jia S, Tian J, Niu Z. Flexible and tailorable quasi-solid-state rechargeable Ag/Zn microbatteries with high performance. *Carbon Energy* 2021;3:167-75. DOI
97. Zhao J, Sonigara KK, Li J, et al. A Smart flexible zinc battery with cooling recovery ability. *Angew Chem Int Ed Engl* 2017;56:7871-5. DOI PubMed
98. Jin X, Song L, Dai C, et al. A flexible aqueous zinc-iodine microbattery with unprecedented energy density. *Adv Mater* 2022;34:e2109450. DOI PubMed
99. Wang S, Jiao S, Song W, et al. A novel dual-graphite aluminum-ion battery. *Energy Storage Mater* 2018;12:119-27. DOI
100. Komaba S, Murata W, Ishikawa T, et al. Electrochemical Na insertion and solid electrolyte interphase for hard-carbon electrodes and application to Na-Ion batteries. *Adv Funct Mater* 2011;21:3859-67. DOI
101. Parker JF, Chervin CN, Pala IR, et al. Rechargeable nickel-3D zinc batteries: an energy-dense, safer alternative to lithium-ion.

Science 2017;356:415-8. DOI PubMed

102. Yirka B. Phinergy demonstrates aluminum-air battery capable of fueling an electric vehicle for 1000 miles. Available from: https://phys.org/news/2013-03-phinergy-aluminum-air-battery-capable-fueling.html [Last accessed on 30 May 2022].
103. Cheong WH, Oh B, Kim S, et al. Platform for wireless pressure sensing with built-in battery and instant visualization. *Nano Energy* 2019;62:230-8. DOI
104. Park J, Ahn DB, Kim J, et al. Printing of wirelessly rechargeable solid-state supercapacitors for soft, smart contact lenses with continuous operations. *Sci Adv* 2019;5:eaay0764. DOI PubMed PMC
105. An HS, Park YG, Kim K, Nam YS, Song MH, Park JU. High-resolution 3D printing of freeform, transparent displays in ambient air. *Adv Sci (Weinh)* 2019;6:1901603. DOI PubMed PMC
106. Zhu M, Schmidt OG. Tiny robots and sensors need tiny batteries - here's how to do it. *Nature* 2021;589:195-7. DOI PubMed
107. Um H, Choi K, Hwang I, Kim S, Seo K, Lee S. Monolithically integrated, photo-rechargeable portable power sources based on miniaturized Si solar cells and printed solid-state lithium-ion batteries. *Energy Environ Sci* 2017;10:931-40. DOI
108. Hu B, Wang X. Advances in micro lithium-ion batteries for on-chip and wearable applications. *J Micromech Microeng* 2021;31:114002. DOI
109. Ren J, Li L, Chen C, et al. Twisting carbon nanotube fibers for both wire-shaped micro-supercapacitor and micro-battery. *Adv Mater* 2013;25:1155-9, 1224. DOI PubMed
110. Wang Y, Chen C, Xie H, et al. 3D-Printed All-Fiber Li-Ion Battery toward Wearable Energy Storage. *Adv Funct Mater* 2017;27:1703140. DOI
111. Hu L, Wu H, La Mantia F, Yang Y, Cui Y. Thin, flexible secondary Li-ion paper batteries. *ACS Nano* 2010;4:5843-8. DOI PubMed
112. Zheng S, Wu Z, Zhou F, et al. All-solid-state planar integrated lithium ion micro-batteries with extraordinary flexibility and high-temperature performance. *Nano Energy* 2018;51:613-20. DOI
113. Nasreldin M, Mulatier S, Delattre R, Ramuz M, Djenizian T. Flexible and stretchable microbatteries for wearable technologies. *Adv Mater Technol* 2020;5:2000412. DOI
114. Wang Z, Mo F, Ma L, et al. Highly Compressible cross-linked polyacrylamide hydrogel-enabled compressible Zn-MnO_2 battery and a flexible battery-sensor system. *ACS Appl Mater Interfaces* 2018;10:44527-34. DOI PubMed
115. Liu N, Zhou G, Yang A, et al. Direct electrochemical generation of supercooled sulfur microdroplets well below their melting temperature. *Proc Natl Acad Sci USA* 2019;116:765-70. DOI PubMed PMC
116. Zhou B, He D, Hu J, et al. A flexible, self-healing and highly stretchable polymer electrolyte via quadruple hydrogen bonding for lithium-ion batteries. *J Mater Chem A* 2018;6:11725-33. DOI
117. Yang Y, Wang S, Zhang Y, Wang ZL. Pyroelectric nanogenerators for driving wireless sensors. *Nano Lett* 2012;12:6408-13. DOI PubMed